# Development and characterization of a stable adhesive bond between a poly(dimethylsiloxane) catheter material and a bacterial biofilm resistant acrylate polymer coating

Bonnie J. Tyler[a)]
*Physikalisches Institut, University of Münster, 48159 Münster, Germany*

Andrew Hook
*School of Pharmacy, University of Nottingham, NG7 2RD Nottingham, United Kingdom*

Andreas Pelster
*Physikalisches Institut, University of Münster, 48159 Münster, Germany*

Paul Williams
*Centre of Biomolecular Sciences, School of Life Sciences, University of Nottingham, NG7 2RD Nottingham, United Kingdom*

Morgan Alexander
*School of Pharmacy, University of Nottingham, NG7 2RD Nottingham, United Kingdom*

Heinrich F. Arlinghaus
*Physikalisches Institut, University of Münster, 48159 Münster, Germany*

(Received 15 March 2017; accepted 10 May 2017; published 23 May 2017)

Catheter associated urinary tract infections are the most common health related infections worldwide, contributing significantly to patient morbidity and mortality and increased health care costs. To reduce the incidence of these infections, new materials that resist bacterial biofilm formation are needed. A composite catheter material, consisting of bulk poly(dimethylsiloxane) (PDMS) coated with a novel bacterial biofilm resistant polyacrylate [ethylene glycol dicyclopentenyl ether acrylate (EGDPEA)-*co*-di(ethyleneglycol) methyl ether methacrylate (DEGMA)], has been proposed. The coated material shows excellent bacterial resistance when compared to commercial catheter materials, but delamination of the EGDPEA-*co*-DEGMA coatings under mechanical stress presents a challenge. In this work, the use of oxygen plasma treatment to improve the wettability and reactivity of the PDMS catheter material and improve adhesion with the EGDPEA-*co*-DEGMA coating has been investigated. Argon cluster three dimensional-imaging time-of-flight secondary ion mass spectrometry (ToF-SIMS) has been used to probe the buried adhesive interface between the EGDPEA-*co*-DEGMA coating and the treated PDMS. ToF-SIMS analysis was performed in both dry and frozen-hydrated states, and the results were compared to mechanical tests. From the ToF-SIMS data, the authors have been able to observe the presence of PDMS, silicates, salt particles, cracks, and water at the adhesive interface. In the dry catheters, low molecular weight PDMS oligomers at the interface were associated with poor adhesion. When hydrated, the hydrophilic silicates attracted water to the interface and led to easy delamination of the coating. The best adhesion results, under hydrated conditions, were obtained using a combination of 5 min $O_2$ plasma treatment and silane primers. Cryo-ToF-SIMS analysis of the hydrated catheter material showed that the bond between the primed PDMS catheter and the EGDPEA-*co*-DEGMA coating was stable in the presence of water. The resulting catheter material resisted *Escherichia coli* and *Proteus mirabilis* biofilm colonization by up to 95% compared with uncoated PDMS after 10 days of continuous bacterial exposure and had the mechanical properties necessary for use as a urinary catheter. © *2017 American Vacuum Society*. [http://dx.doi.org/10.1116/1.4984011]

## I. INTRODUCTION

Catheter associated urinary tract infections (CA-UTIs) are the most common health care related infections worldwide[1] with an estimated symptomatic infection of 100 000 annually in the USA alone.[2,3] These CA-UTIs result in an increased length of hospital stays with associated costs,[4] contribute to the development of drug resistant bacterial strains,[3] and lead to increased mortality.[5,6] Bacterial biofilm formation on the interior and exterior surfaces of the catheter has been identified as the most important cause of CA-UTIs.[7,8] To reduce the incidence of these infections, there is a critical need for new catheter materials that prevent bacterial biofilm formation. Using a combinatorial polymer library, Hook *et al*. have identified a bacterial biofilm resistant polyacrylate, a copolymer of ethylene glycol dicyclopentenyl ether acrylate (EGDPEA) and di(ethyleneglycol) methyl ether methacrylate (DEGMA), that is resistant to bacterial attachment in both *in vitro* and

[a)]Electronic mail: tyler@uni-muenster.de

*in vivo* assays.[9,10] This copolymer has mechanical properties compatible with a flexible coating on poly(dimethylsiloxane) (PDMS) necessary for many medical device applications such as catheters.[11]

PDMS has the flexibility, inertness, and durability required for urinary catheters as well as a range of other biomedical applications such as breast prosthesis, hydrocephalus shunts, cardiac pacemakers, cochlear implants, artificial skins, temporomandibular joints, drug delivery systems, drainage implants in glaucoma, maxillofacial reconstruction, esophagus replacements, finger joints, and denture liners. Despite its excellent bulk properties, the surface properties of PDMS frequently lead to an adverse biological response such as fibrotic encapsulation, thrombosis, or bacterial biofilm formation.[12–14] For this reason, there have been many efforts to modify the surface of PDMS in order to improve the induced biological response. In this work, we have investigated coating PDMS catheter tubing with the EGDPEA-*co*-DEGMA coating to create a catheter material that would be resistant to bacterial biofilm formation.

Creating a strong adhesive bond between PDMS and any coating is difficult because of the inertness and hydrophobicity of PDMS. A number of strategies have been employed to modify the surface of PDMS, such as blending, copolymerization, interpenetrating polymer networks, and functionalization.[15,16] In this work, we have used $O_2$ plasma treatment of PDMS to improve the hydrophilicity and reactivity of the surface. Plasma treatment has been previously used to reduce the hydrophobicity of PDMS, hence making it more favorable for cell attachment. In particular, the $O_2$ plasma has been extensively investigated for producing a thin silica sheet on PDMS, providing a hydrophilic layer that can prevent solvent swelling, improve wetting, and inhibit the migration of PDMS oligomers to the surface. In addition to producing a silica layer, plasma treatment is well known for its ability to produce long-lived, highly reactive radicals within treated species.[17] These groups can be advantageous for establishing covalent links between a coating and the PDMS or for inducing subsequent grafting-to polymerization.[18] In this study, we explore the influence of $O_2$ plasma treatment on PDMS for improving the interaction of an antibacterial coating[9,10] with PDMS catheter tubing.

Historically, studying adhesion between polymer layers has been extremely challenging because of a lack of suitable analytical techniques for probing the buried interface. Recent advances in cluster ion beam technology have made sputter depth profiling a practical alternative for 3D imaging of organic materials.[19–23] In this work, we have used dual-beam 3D imaging time-of-flight secondary ion mass spectrometry (ToF-SIMS),[24] using an argon cluster sputter source, to probe the adhesive layer between the EGDPEA-*co*-DEGMA coating and a PDMS catheter in order to better understand and thereby improve the adhesion.

## II. METHODS

### A. Polymer preparation

To prepare the polymer, bis[(difluoroboryl)diphenyl glyoximato]cobalt(II) (CoPhBF, 1000 ppm) and 2,2′-azobis (4-methoxy-2,4-dimethylvaleronitrile) (0.5%, w/v) were added to monomers EGDPEA and DEGMA; EGDPEA: DEGMA = 3:1 in toluene. The chemical structure of the monomers is shown in Fig. S1 in the supplementary material.[37] The ratio between monomers and toluene was 1:4. The solution was degassed using at least two freeze-pump-thaw cycles, until no more bubble formation was observed in the thaw step. The polymerization was conducted at 80 °C for 24 h under $N_2$. The polymerization was terminated by exposure to air and cooling the reaction flask. $^1$H and $^{13}$C nuclear magnetic resonance spectra were acquired in deuterated chloroform on both Bruker DPX (300 MHz) and AV (400 MHz) instruments. The number-average molecular weight (Mn), weight-average molecular weight (Mw), and polydispersity were obtained by gel permeation chromatography with a fitted IR detector. Polymer samples (7 mg/ml) dissolved in tetrahydrofuran were flown (1 ml/min) through a PLgel 5 mm guard column (Polymer Laboratories) and two PLgel 5 mm MIXED-C columns (Polymer Laboratories) at 40 °C. The polymer was precipitated by dropwise addition to cold hexane. The polymer was dried under vacuum (<50 mbar) overnight before use.

### B. Sample preparation

PDMS tubing (Sterilin) of 100% was cut into approximately 10 mm lengths, washed with acetone for 10 min by sonication, dried, and then $O_2$ plasma treated using a custom built reactor as shown in Fig. 1. The reactor pressure was initially reduced to below 0.02 mbar and flushed twice with $O_2$ before plasma treatment. For plasma treatment, the initial $O_2$ pressure was 0.4 mbar and the typically running pressure was 0.49–0.58 mbar. Plasma treatment times were 10 s, 1, 5, 10, and 30 min. The plasma power was 100 W. After plasma treatment was completed, the chamber was evacuated to

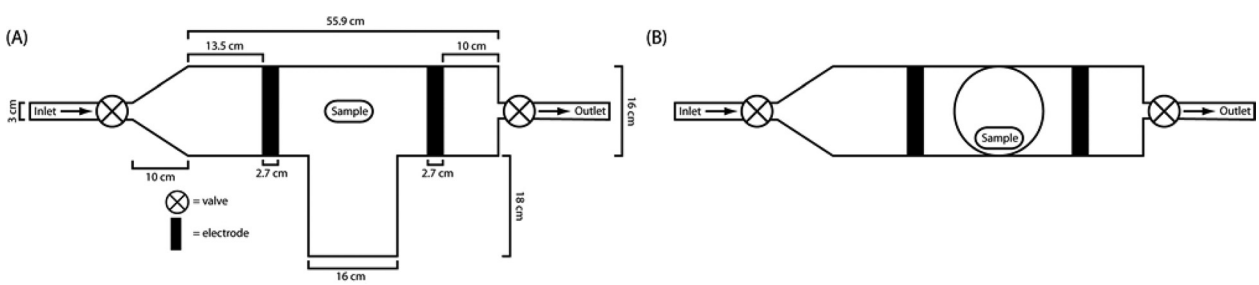


FIG. 1. Schematic depiction of the plasma reactor: (a) top view and (b) side view.

below 0.08 mbar before exposure to the atmosphere. The treated samples were then immersed for 10 min into 7.5% (w/v) polymer solution in dichloromethane within 2 min from the end of the plasma cycle. Samples were then withdrawn at approximately 5 mm/s, blotted and dried overnight at ambient conditions, and then dried in vacuum (<50 mbar) at 75 °C for 3 days.

Silane primed samples were prepared by immersing PDMS tubing (Sterilin) into a 20% (v/v) mixture of tetrabutyl-titanate, tetrapropylsilicate, and tetra(2-methoxyethoxy)silane in naphtha solvent (Nusil MED1-161). Samples were withdrawn at approximately 1 mm/s and allowed to dry for 5 min before dipping into 7.5% (w/v) polymer solution in dichloromethane. Samples were then withdrawn at approximately 5 mm/s, blotted and dried overnight at ambient conditions, and then dried in vacuum (<50 mbar) at 75 °C for 3 days.

### C. Sample analysis

The coating thickness was determined gravimetrically by weighing samples before and after coating using a microbalance. The mass of the coating was determined as the difference between the two measurements and was converted into a volume (polymer density = 1.6 g/ml). The coating thickness was determined by dividing the coating volume by the surface area of the sample, which included internal and external faces and as well as both the ends of a sample. For measurements of the water contact angle (WCA), a CAM200 instrument (KSV Instruments, Ltd) was used to dispense 10 $\mu$l volume sessile water droplets onto plasma treated PDMS samples. Three measurements were taken per sample. Ultrapure water was used for all the CA measurements (18.2 MΩ resistivity at 25 °C). WCA measurements after $O_2$ plasma treatment were taken within 2–4 min of the completion of the plasma treatment cycle. Light microscopy images were acquired using an Olympus IX51 microscope and a Smart Imaging System (IMSTAR S.A.) with a 10× objective lens. Scanning electron microscopy images were acquired using a JSM 6400 Scanning Microscope (JEOL WinSem). Samples were fixed onto conductive carbon tape and precoated with an approximately 10 nm Pt layer prior to imaging. To obtain cross-sectional images, samples were immersed into liquid nitrogen and then fractured using a scalpel blade.

### D. Revolution-to-delamination assay

To assess the strength of the interface between the polymer coating and the PDMS substrate, coated samples were subjected to a rolling tube compression test which puts very stringent interfacial stresses upon the interfaces. The output from this was the number of revolution to delamination (RTD), which could be compared as a measure of interfacial stability. This test was performed by placing the samples between two glass slides, and a 1 kg weight was placed on top of the sample (see supplementary material, Fig. S2).[37] The bottom glass slide was fixed, whilst the top slide was moved back and forth to cause the sample to roll along the two glass surfaces. The sample was rolled until a complete revolution was completed, and then the movement direction was reversed. This was continued until a delamination event was observed or 1000 rotations were completed. Between samples both the glass surfaces were thoroughly cleaned with isopropanol. For the analysis of hydration effects, samples were placed into ultrapure water (18.2 MΩ resistivity at 25 °C) for 1 h. Samples were then blotted onto a paper towel to remove excess water from the lumen of the sample and then rolled once to remove excess water from the exterior of the sample.

### E. Bacterial attachment assay

Uropathogenic *Escherichia coli* (UPEC) (*E. coli* 536)[25] and *Proteus mirabilis* (DSMZ226637, clinical isolate, Queens Medical Centre, UK) were routinely grown on either Luria-Bertani (Oxoid, UK) agar plates at 37 °C or in broth at 37 °C with 200 rpm shaking. RPMI-1640 chemically defined medium (Sigma, UK) was used in the biofilm experiments. For comparison, bacterial attachment to untreated PDMS and silver hydrogel coated latex catheters (BactiGuard, Bardex) was also assessed. Prior to incubation with the bacteria, the samples were UV sterilized and washed with phosphate buffer saline (PBS, Oxoid) for 10 min. Bacteria were grown on polymer samples under similar conditions to those previously described.[10] Briefly, samples were incubated in 10 ml of medium inoculated with diluted ($OD_{600} = 0.01$) bacteria from overnight cultures and grown at 37 °C with 60 rpm shaking for 3–10 days. After 3 days of growth, the media were decanted and replaced with 10 ml of fresh, prewarmed media. As growth medium controls, samples were also incubated without bacteria. At the desired time points, the samples were removed, washed three times with 15 ml of PBS at room temperature for 5 min at 60 rpm, rinsed with distilled $H_2O$, and stained with 20 $\mu$M SYTO17 dye (Invitrogen, UK) at room temperature for 30 min. After air drying, the samples were examined using a Carl Zeiss LSM 700 Laser Scanning Microscope with ZEN 2009 imaging software (Carl Zeiss, Germany). The coverage of bacteria on the surface was analyzed using open source Image J 1.44 software (National Institute of Health, USA).

### F. ToF-SIMS analysis

ToF-SIMS measurements were performed on a custom built ToF-SIMS instrument, which are largely comparable to the IONTOF V. The instrument is equipped with a novel cryo-preparation chamber to allow easy handling of frozen hydrated samples. The 3D images of the catheters were obtained in the dual beam mode using an analysis area of $100 \times 100\ \mu m^2$ and a sputter area of $500 \times 500\ \mu m^2$. Analysis was performed with a 0.05 pA (pulsed mode) 30 keV $Bi_3^+$ primary ion beam, and sputtering was done with a 2.1 nA, 10 keV $Ar_{2000}^+$ beam. Noninterlaced sputtering, with a 50 s analysis cycle, 20 s sputter cycle, and 1 s pause, was used to minimize sample charging, resulting in an analysis beam

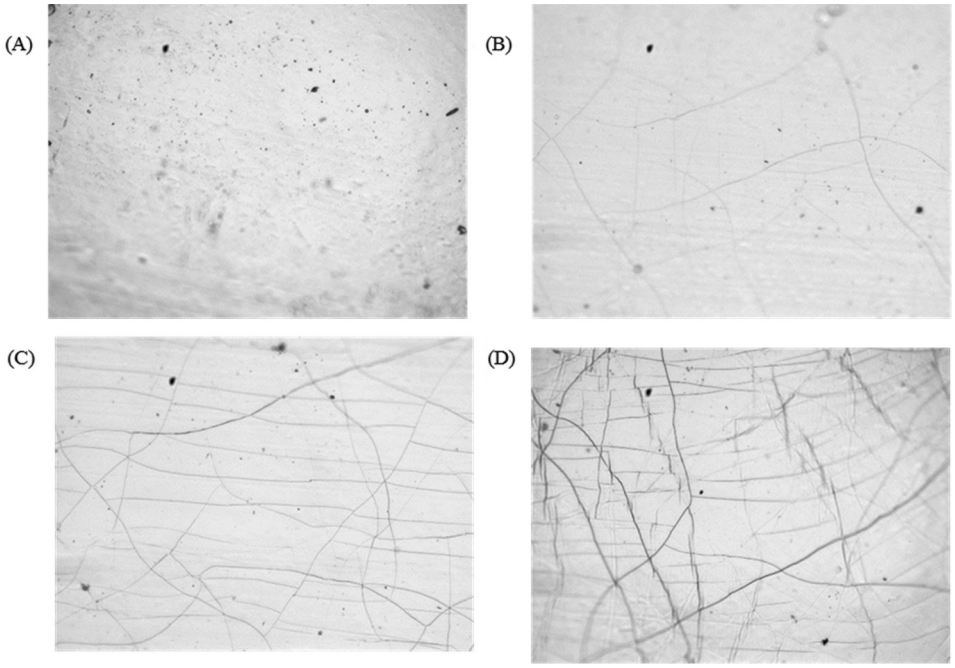


FIG. 2. Bright field light microscopy images of PDMS after oxygen plasma treatment. Treatment times were (a) as received, (b) 5 min, (c) 10 min, and (d) 30 min.

dose density per cycle of 0.0015 ions/nm$^2$ and a sputter dose density per cycle of 1.0 ions/nm$^2$.

To study hydration effects, samples were submerged in ultrapure water for >1 h. The samples were then blotted dry, mounted on a copper stub, and plunge-frozen in liquid nitrogen. Freezing was performed inside a glove box and transferred to the ToF-SIMS cryo-preparation chamber under a nitrogen atmosphere to prevent the formation of a frost layer on the surface. Once transferred to the instrument, the samples were maintained below −120 °C throughout the analysis process.

## III. RESULTS AND DISCUSSION

### A. Plasma treatment of PDMS

PDMS samples were initially exposed to $O_2$ plasma treatment at a power of 100 W from 10 s to 30 min. After treatment, samples were assessed by light microscopy and WCA. Figure 2 shows the light micrographs of untreated PDMS [Fig. 2(a)] and samples treated with the $O_2$ plasma for 5 min [Fig. 2(b)], 10 min [Fig. 2(c)], and 30 min [Fig. 2(d)]. No change in the appearance of samples was observed after plasma treatment for 10 s or 1 min compared with untreated PDMS. After 5 min of treatment, cracks were observed on the PDMS surface [Fig. 2(b)]. The number of cracks increased with further treatment [Figs. 2(c) and 2(d)]. Crack formation has previously been observed after plasma treatment of PDMS due to the formation of a brittle silica layer, which becomes thicker with longer treatment.[14,26–28]

Figure 3 shows water contact angle measurements for the plasma treated PDMS immediately (2–4 min) following plasma treatment. Immediately following plasma treatment, the WCA decreased from 116° ± 2° to 65° ± 2° for samples that were plasma treated between 1 and 10 min. For the 30 min plasma treatment, a higher WCA of 91° ± 3° was observed, which correlated with increased cracking of the sample surface. After 1 week, the WCA of all the samples (data not shown) was within the measurement error of the untreated PDMS. Hydrophobic recovery of treated PDMS has been previously observed in many studies and has been attributed to the migration of lower molecular weight PDMS oligomers from the bulk to the surface.

### B. Substrate coating

Within 5 min after plasma treatment, the catheter tubing was dip-coated with EGDPEA-*co*-DEGMA. Once dried, all

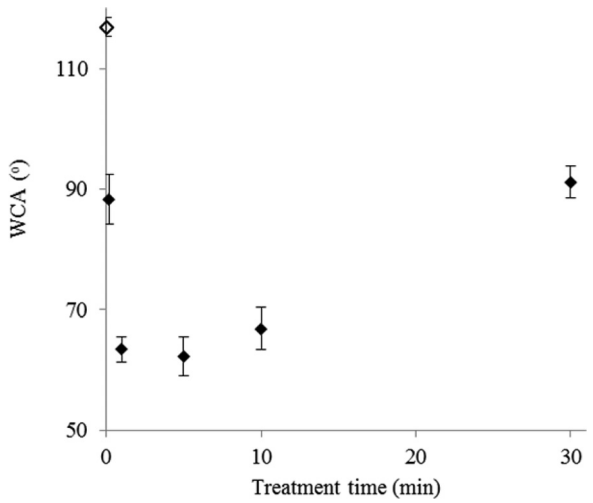


FIG. 3. Change in WCA of the oxygen plasma treated time immediately after plasma treatment. The unfilled symbol indicates untreated PDMS.

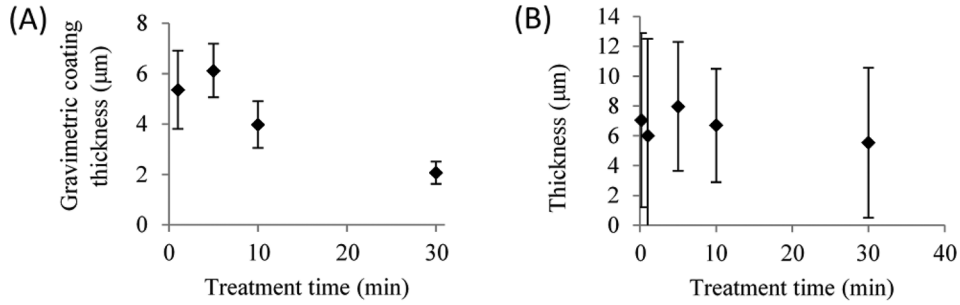


FIG. 4. Coating thickness as determined by gravimetric analysis (a) and SEM measurements (b). Error bars equal ±1 standard deviation unit, n = 5.

coatings on plasma treated PDMS appeared smooth and homogeneous. In contrast, coatings on untreated PDMS dewetted on the surface. The shortest treatment time (10 s) was thus sufficient to avoid dewetting of the coating. The coating thickness was determined by gravimetric analysis and SEM measurements and is shown in Fig. 4. Representative SEM images are shown in Fig. S3 of the supplementary material.[37] A maximum thickness of $7 \pm 1\ \mu$m was observed for the 5 min treatment time. The coating thickness decreased with an increase in treatment time to a minimum thickness of $2 \pm 0.5\ \mu$m for the 30 min treatment [Fig. 4(a)]. SEM measurements of the coating thickness [Fig. 4(b)], however, show large variability (std $> \pm 4\ \mu$m) in the coating thickness for all treatment times. SEM data showed no statistically significant difference in the coating thickness on samples with different plasma treatment times. However, by gravimetric analysis, a statistically significant ($p < 0.05$) decrease in the coating thickness was observed for coatings on the sample plasma treated for 30 min. It should be noted that the gravimetric analysis measures an average thickness across the whole sample, whereas the SEM measurements are associated with the localized regions of the sample.

## C. Mechanical testing

Figure 5 shows the result of the RTD test for dry and hydrated samples. Examples of delamination events are shown in the supplementary material (Fig. S3).[37] For dry samples, the RTD increased from less than 10 for treatment times under 5 min to >1000 for treatment times over 10 min [Fig. 5(a)]. Note that the test was stopped after 1000 revolutions if no delamination occurred, and so, the apparent plateau in Fig. 5 is artificial. A dramatic reduction in adhesion was observed after hydration, with the maximum RTD of $12 \pm 7$ occurring for a treatment time of 5 min, a statistically significant ($p < 0.05$) increase compared with the RTD measured for samples with treatment times of 10 s or 10 min. This suggests that this treatment time produced sufficient reactivity at the PDMS surface to ensure adhesion between the coating and the catheter without excessive production of a silica layer. Further increasing the treatment time to 10 min decreased the RTD to 2 revolutions, and a further decrease to 0.5 revolutions was observed for a treatment time of 30 min.

## D. Bacterial attachment assay

A treatment time of 5 min was selected for bacterial attachment studies because it showed the best resistance to delamination under hydrated conditions. These coatings were subjected to bacterial attachment assays using UPEC and *P. mirabilis* for 3–10 days. These two bacterial strains are highly relevant in catheter associated urinary tract infections.[29,30] The results of the bacterial attachment assay are shown in Fig. 6. After 3 days of culturing [Fig. 6(a)], bacterial coverage on poly(EGDPEA-*co*-DEGMA) was <3% and <1.5% for *P. mirabilis* and UPEC, respectively. This is comparable with the *P. mirabilis* coverage of >17% and the UPEC coverage of >6% for the untreated and silver hydrogel controls. The low bacterial coverage on the EGDPEA-*co*-DEGMA coating

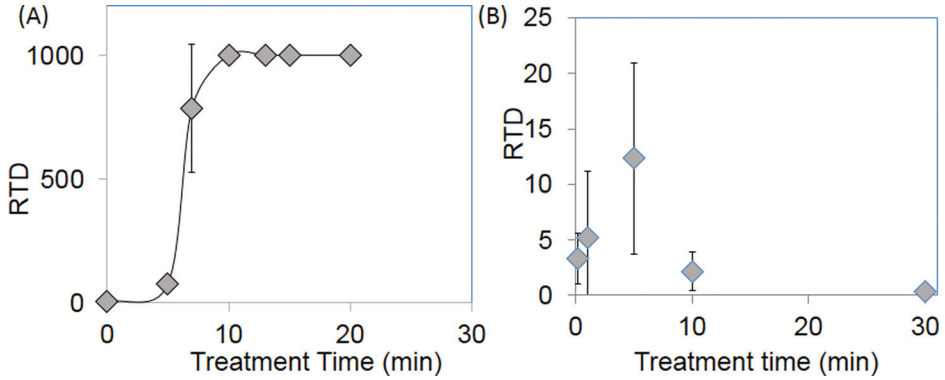


FIG. 5. RTD observed for various $O_2$ plasma treatment times for dry (a) and hydrated (b) EGDPEA-*co*-DEGMA coated PDMS catheter samples. Error bars equal ±1 standard deviation unit, n = 5.

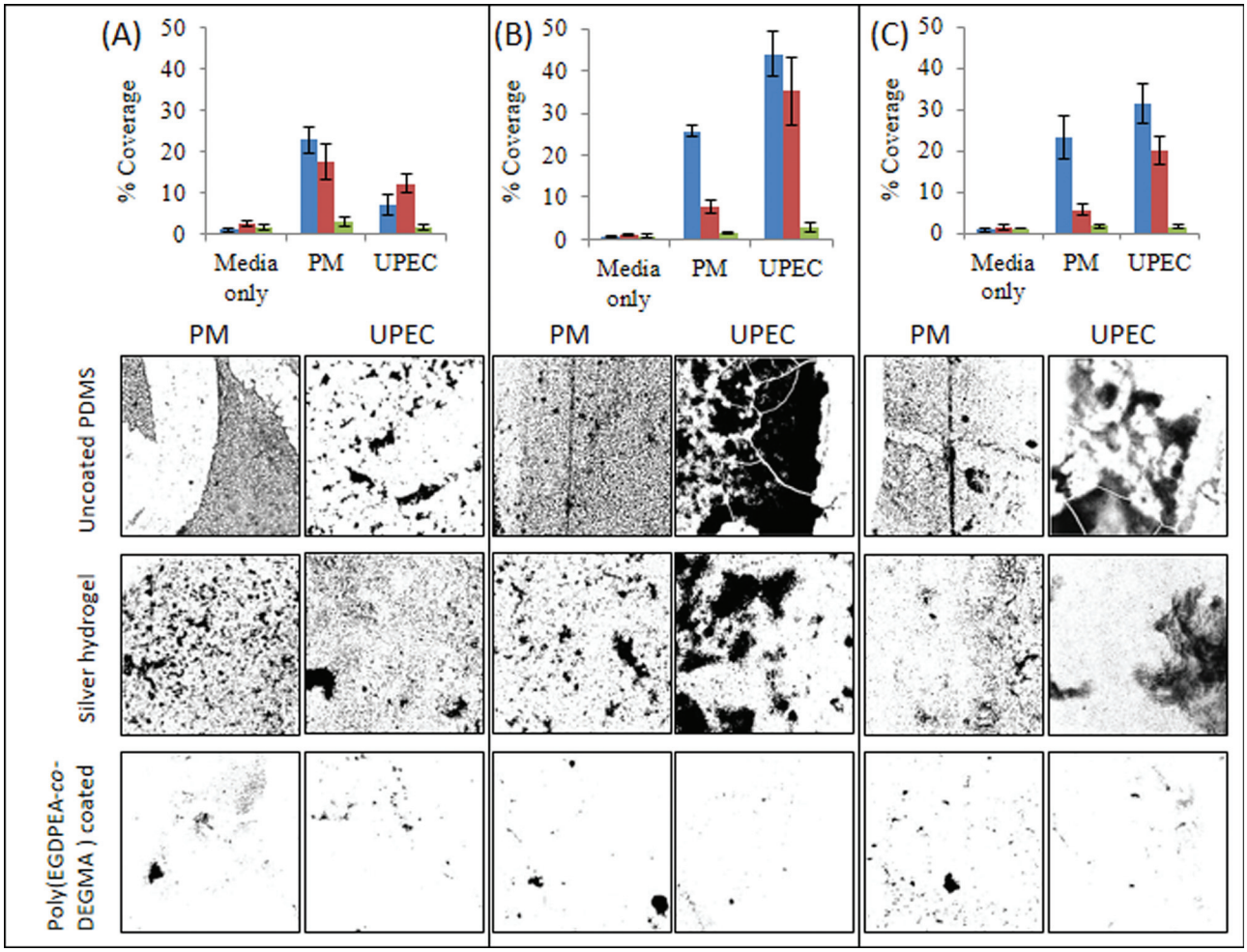


FIG. 6. Summary of bacterial attachment onto uncoated PDMS (blue square), silver hydrogel (red square), and poly(EGDPEA-*co*-DEGMA) coated PDMS (green square). Analysis was performed after (a) 3, (b) 6, or (c) 10 days of culturing of samples with *P. mirabilis* (PM) and UPEC. Bacterial coverage (top) was calculated on SYTO64 stained samples. Three images were acquired from each sample, and three repeated samples were assessed for each time point/same type. Error bars equal $\pm 1$ standard deviation unit, $n = 9$. The representative maximum z-projection images for each substrate and bacterial species are shown. Images are $640 \times 640\ \mu m^2$.

was maintained for the entire incubation period of 10 days (Fig. 6). Samples showed no signs of delamination throughout this period, demonstrating that the oxygen plasma treatment produced a sufficiently strong interface between the coating and PDMS to prevent delamination in an aqueous environment. On the untreated PDMS, the *P. mirabilis* coverage remained steady at approximately 23% for the 10 day period, whilst the UPEC coverage increased from 6% to >30% from 3 to 10 days of incubation. After 3 days, the *P. mirabilis* coverage on the silver hydrogel was >17%; however, this decreased to approximately 5% after 10 days, suggesting that the silver hydrogel may have been able to kill this bacterial species over the time course of the experiment. The UPEC coverage on the silver hydrogel catheter fluctuated throughout the experiment within the range of 12%–35%. In summary, the EGDPEA-*co*-DEGMA coating achieved a reduction between 86% and 95% in bacterial coverage (*P. mirabilis* and UPEC) compared with untreated PDMS and between 66% and 93% compared with the silver hydrogel after 10 days of continuous bacterial exposure.

### E. ToF-SIMS analysis

Replicate ToF-SIMS 3D-images were collected on $100 \times 100\ \mu m$ areas on the 5, 10, and 30 min 100 W $O_2$ treated samples. The sputter time required to reach the interface varied significantly within each sampled region, indicating nonuniformity in either the coating thickness or the sputter yield. This nonuniform layer thickness led to the poor resolution of the interface. To improve the resolution of the interface, all the 3D images were corrected to align the layers at the base of the polymer layer.[31,32] Alignment was done using an autocorrelation function rather than a threshold, as this proved to be less sensitive to noise. Note that this pixel level realignment of the ToF-SIMS profiles was intended to improve the resolution of the interface rather than produce realistic 3D images. The images were processed using principal component analysis and the multivariate curve resolution to identify all the major components. Three major components, EGDPEA-*co*-DEGMA, silicate, and PDMS, were identified in all the sampled regions. Additionally, dust particles rich in $Na^+$, $K^+$, and $NH_4^+$ were observed at the interface

between the polymer film and the catheter in many of the regions. ToF-SIMS spectra of these components are provided in the supplementary material (Fig. S5).[37] Salt rich particles are common components of ambient aerosol,[33,34] and their presence at the interface suggests that they were most likely present on the catheter surfaces prior to plasma treatment and EGDPEA-*co*-DEGMA coating.

Representative depth profiles and 3D images of samples treated for 5, 10, and 30 min are shown in Fig. 7. The signals shown are the sum of characteristic peaks determined from the multivariate analysis. A table summarizing these peaks is provided in the supplementary material (Table S1).[37] The unusual drop in the EGDPEA-*co*-DEGMA signal in the depth profiles, at the outermost surface of the samples, is an artefact of the topographic correction of the data. For all the images, the EGDPEA-*co*-DEGMA layer is shown in blue, silicate is shown in green, and PDMS is shown in red. All the samples show traces of PDMS contamination at the outermost surface on top of the EGDPEA-*co*-DEGMA coating.

For the 5 min treated sample [Figs. 7(a) and 7(b)], four layers were identified, the top layer of EGDPEA-*co*-DEGMA, followed by an ultrathin layer of pure oligomeric PDMS, a layer of mixed silicate and PDMS, and then the bulk cross-linked PDMS catheter material. The sputter ion yield for silicates with argon cluster beams is 2–3 orders of magnitude lower than that for common polymeric materials. The fact that it was possible to sputter quickly through the silicate layer suggests that the layer was very thin and/or only lightly oxidized, which is consistent with the low degree of cracking seen in the optical micrographs. The

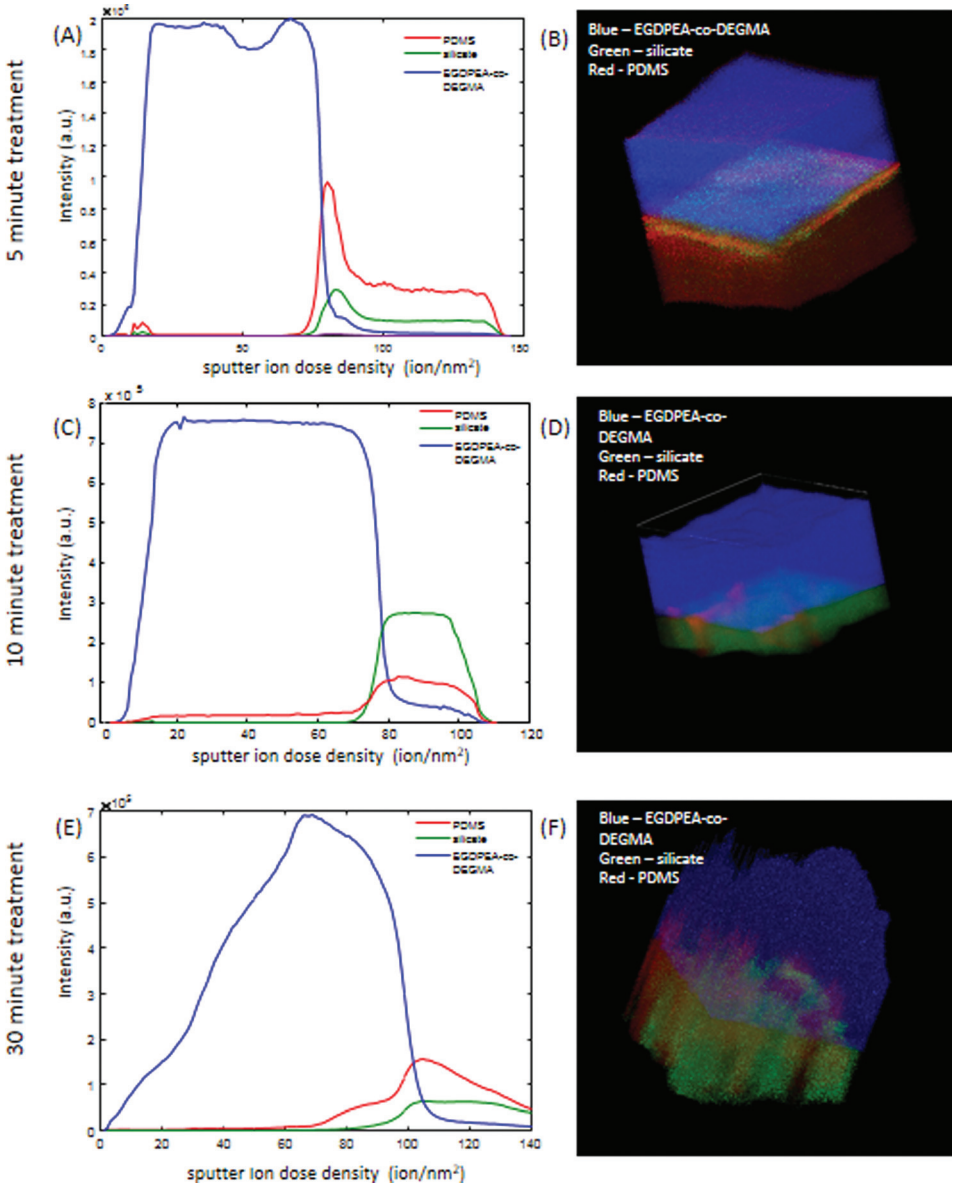


FIG. 7. ToF-SIMS depth profiles and 3D images of $100 \times 100\,\mu$m regions on EGDPEA-*co*-DEGMA coated PDMS catheters that were treated for 5 min. [(a) and (b)], 10 min [(c) and (d)], and 30 min [(e) and (f)] with the $O_2$ plasma. EGDPEA-*co*-DEGMA is shown in blue, silicate in green, and PDMS in red. The depth scale is uncalibrated. The intensity is in arbitrary units.

increase in the amount of PDMS at the interface relative to the bulk catheter indicates that this area is dominated by highly mobile low molecular weight PDMS oligomers that give a more intense SIMS signal than the crosslinked polymer. The presence of the low molecular weight PDMS at the interface is consistent with the relatively low dry measured mechanical strength of this sample.

In the samples treated for 10 and 30 min [Figs. 7(c)–7(f)], the depth profile ends in the silicate layer, and so, the bulk PDMS catheter is never reached, indicating a thicker and/or harder silicate layer that is difficult to sputter. In the 10 min treated sample, [Figs. 7(c) and 7(d)] only two layers are observed, the EGDPEA-*co*-DEGMA film and a mixed silicate/PDMS layer. The PDMS signal rises only after the silicate signal appears [Fig. 7(c)] and is observed along well defined cracks in the silicate layer [Fig. 7(d)].

In contrast to the 10 min treated sample, the PDMS signal in the 30 min treated sample begins to increase well before the silicate signal appears [Fig. 7(e)], indicating the presence of an intermediate layer of mixed PDMS/EGDPEA-*co*-DEGMA. The 3D image [Fig. 7(f)] shows that this PDMS/EGDPEA-*co*-DEGMA layer is not uniform across the surface but is localized to particular spots. In the regions where the PDMS extends up into the EGDPEA-*co*-DEGMA film, both EGDPEA-*co*-DEGMA and PDMS are present, indicating that the two polymers are mixed at the lateral resolution of the SIMS measurement (2–3 $\mu$m). Note that these mixed layers could be protruding down into cracks in the silicate layer rather than upward into the EGDPEA-*co*-DEGMA. It is impossible to distinguish between these two possibilities from the SIMS measurement alone. The presence of PDMS between the polymer and the silicate layer is consistent with the higher water contact angle measured on this sample. From the 3D image [Fig. 9(b)], it is evident that the EGDPEA-*co*-DEGMA layer in this sample has more variations in the thickness than the previous samples. In general, the film is thinner in areas where there is more PDMS at the interface. This is consistent with the thinner average thickness determined by gravimetric analysis.

Figure 8 shows the side-by-side comparison of the interface region (100 × 100 $\mu$m) for the same 5, 10, and 30 min plasma treated samples shown in Fig. 7. In all the three images, PDMS is shown in red, silicate is shown in green, and salt-rich dust particles are shown in blue. The morphology of the interface in the 5 min treated sample [Fig. 8(a)] differs distinctly from those obtained from the longer treatments. The silicate layer is not only thinner and more easily sputtered but also patchy, and PDMS is visible across most of the interface. After the 10 min treatment [Fig. 8(b)], the PDMS appears only along distinct lines with a nearly uniform width of ~10 $\mu$m. After the 30 min treatment [Fig. 8(c)], more interfaces are covered with PDMS and the features are much more irregular in size. Although this set of images shows an increasing number of particles at the interface with increasing plasma exposure time, replicate measurements showed significant region-to-region variability in the particle numbers.

ToF-SIMS images collected following the depth profiles, after the argon cluster sputtering was stopped, showed the rapid migration of the PDMS across the sputter cleaned surface. Figure 9 shows the higher spatial resolution (~500 nm) ToF-SIMS images of the PDMS (m/z = 73 + m/z = 147) signal of the interface of a second 10 min treated area. The image on the left [Fig. 9(a)] was taken within 1 min of Ar cluster sputtering. The image on the right [Fig. 9(b)] was taken 5 min later. As is evident from the images, PDMS migration across the sputter cleaned surface is very rapid with ~85% surface coverage occurring in 5 min. These results suggest that the uniform width of the PDMS lines in the 10 min treated samples [Fig. 8(b)] was the result of PDMS migration from cracks in the silicate during image acquisition between sputter cycles. To confirm this hypothesis, an additional ToF-SIMS depth profile was performed on the 10 min treated catheter, while maintaining the sample at below −120 °C to prevent PDMS migration. In this depth profile (data not shown), PDMS was still observed on the outermost surface, but no PDMS was observed at the EGDPEA-*co*-DEGMA-silicate interface until the sample was allowed to warm up to ambient temperature and migration ensued.

Figure 10 shows the results for ToF-SIMS analysis of the frozen hydrated 10-min-treated catheter. This catheter was

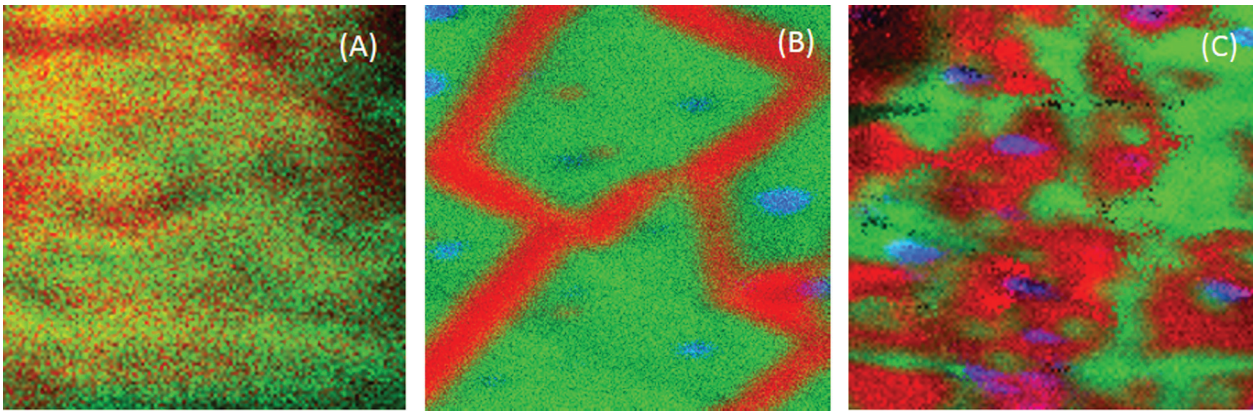


FIG. 8. ToF-SIMS images of 100 × 100 $\mu$m of the interface between the EGDPEA-*co*-DEGMA coating and the plasma treated catheter surface. Samples plasma treated for 5 min (a), 10 min (b), and 30 min (c). Silicate is shown in green, PDMS is shown in red, and dust particles are shown in blue.

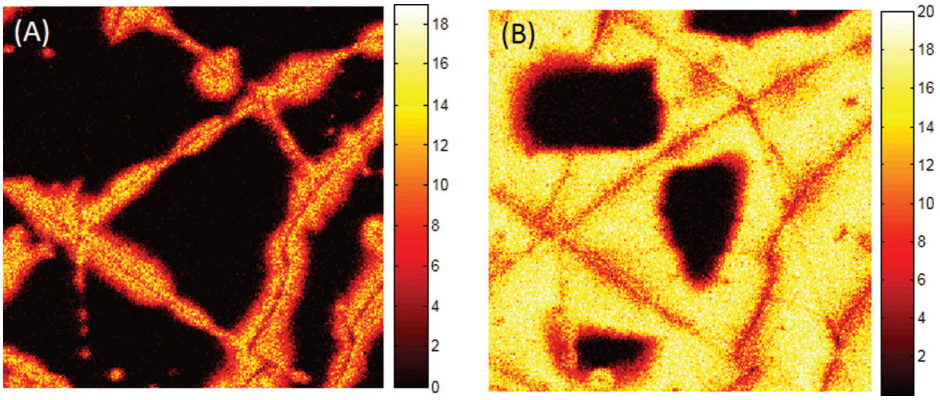


FIG. 9. High spatial resolution 100 × 100 $\mu$m ToF-SIMS images of PDMS (m/z = 73) + (m/z = 147) at the coating/catheter interface taken immediately after 10 keV Ar sputtering (a) and 5 min after sputtering (b) for the sample that had been treated for 10 min with the $O_2$ plasma.

selected for the hydrated analysis because of the large (3 orders of magnitude) drop in RTD in the presence of water. In Fig. 10, EGDPEA-*co*-DEGMA is shown in red, silicate in green, and water in blue. PDMS was not observed either at the surface or the interface of the hydrated sample. Once again, the 3D image has been corrected to align the base of the EGDPEA-*co*-DEGMA layer. As is evident in the depth profile [Fig. 10(a)] and the 3D image [Fig. 10(b)], there is a large film of water between the EGDPEA-*co*-DEGMA layer and the silicate. The image of the interface [Fig. 10(c)] shows beads of water (blue) separated by the cracks in the silicate. Although the EGDPEA-*co*-DEGMA layer itself does not pick up measurable water, water is able to permeate through the film to the hydrophilic interface. A water filled gap is clearly observed between the coating and the PDMS catheter over large portions of the surface, which likely leads to the drop in RTD. The data suggest that water has disrupted the bonding between the coating and the underlying catheter.

Because the mechanical strength of the EGDPEA-*co*-DEGMA/PDMS bond was found to be insufficient using only $O_2$ plasma treatment, we utilized silanization as a methodology for improving interfacial interactions. An additional set of samples was prepared using 5 min $O_2$ plasma treatment followed by priming with a mixture of tetrabutyltitanate, tetrapropylsilicate, and tetra(2-methoxyethoxy)silane in naphtha solvent. The primed coating showed dramatically improved adhesion under hydrated conditions, resisting 1000 rotations before delamination. The EGDPEA-*co*-DEGMA coating on the primed samples was significantly thicker (~25 $\mu$m) than that on the unprimed samples. Figure 11 summarizes the results of the ToF-SIMS measurements on the dry primed sample. EGDPEA-*co*-DEGMA is shown in blue, silicate in green, primer in red, and PDMS in cyan. For simplicity, only the EGDPEA-*co*-DEGMA, silicate, and primer are shown in the 3D image. Although peaks from the organic components of the primer overlapped with the peaks from the polymer and the PDMS, the primer could be clearly identified by its unique titanium signal (see Table S1, supplementary material). The outermost surface of the primed catheter was contaminated with salt particles in all the regions imaged. These particles resulted in artefacts in the profile through the EGDPEA-*co*-DEGMA layer due to differential sputtering. These artefacts are evident in the dark regions in the 3D image and the remnants of EGDPEA-*co*-DEGMA, which persist beyond the interface. Despite these artefacts, the primer, silicate, and PDMS could all be identified in particle free regions of the sample.

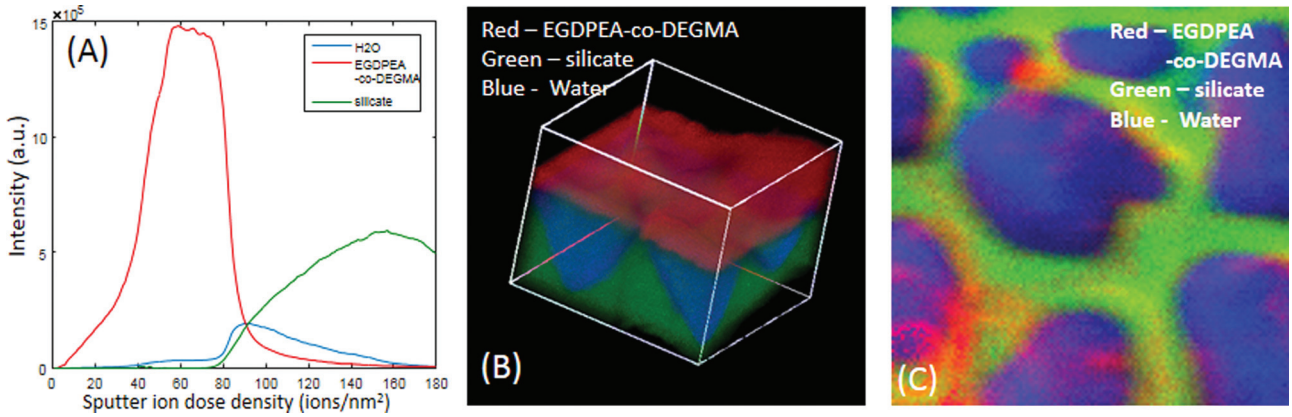


FIG. 10. ToF-SIMS depth profile (a), 3D image (b), and interface image (c) of the 100 × 100 $\mu$m region of the hydrated 10 min treated EGDPEA-*co*-DEGMA coated PDMS catheter. EGDPEA-*co*-DEGMA is shown in red, silicate in green, and water in blue.

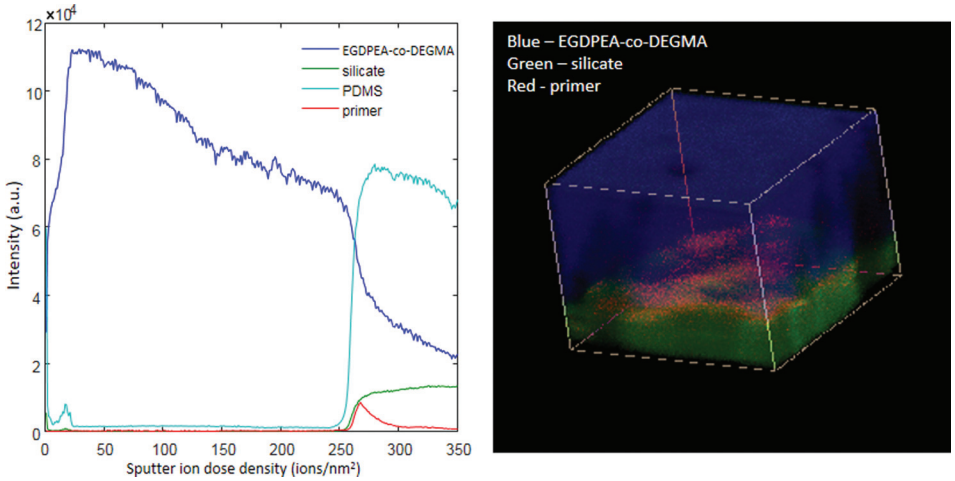


FIG. 11. ToF-SIMS depth profile (a) and 3D image (b) of the 100 × 100 $\mu$m region on the EGDPEA-*co*-DEGMA coated PDMS catheter with the Nusil primer. EGDPEA-*co*-DEGMA is shown in blue, silicate in green, and primer in red. The depth scale is uncalibrated.

Figure 12 summarizes the cryo-ToF-SIMS results for the hydrated primed sample. Note that EGDPEA-*co*-DEGMA is shown in red in the 3D image [Fig. 12(b)], while the primer is shown in red in the interface image [Fig. 12(c)]. Although the primed sample showed significantly improved adhesion when hydrated, trace amounts of water were observed at the interface between EGDPEA-*co*-DEGMA and silicate. These trace amounts of water were localized in a few discrete spots. Detailed analysis of spectra from these water containing regions showed salt and organic impurities that were not observed in the hydrated material without the primer. This suggests that the traces of water were associated with hydrophilic salt particles that were seen at most of the interfaces.

Clear differences in the levels of PDMS at the interface as well as the thickness and morphology of the silicate layer were detected for samples treated with the $O_2$ plasma for 5, 10, and 30 min. The sample treated for 5 min showed higher levels of hydrophobic PDMS at the interface, which could explain both the lower dry RTD values and the lower susceptibility of the adhesive bond to hydration.

The 10 min treated sample showed no PDMS at the interface although PDMS was able to migrate from the bulk to cover the bare silicate surface within a few min, once the EGDPEA-*co*-DEGMA film was removed. Although hydrophobic recovery of plasma-treated PDMS has been widely reported in the literature, it has generally been reported over periods of days not minutes.[27,28,35,36] In this study, hydrophobic recovery on the uncoated plasma treated samples was observed after 1 week, but not in the measurements taken within 5 min of the treatment, in contrast to the SIMS results on sputter cleaned surfaces. This suggests that the rate of hydrophobic recovery is initially determined by the rate of crack propagation through the silicate layer. However, once cracks are formed, low molecular weight PDMS is able to rapidly migrate across the bare silicate surface in only a few min. The application of the EGDPEA-*co*-DEGMA coating immediately after plasma treatment, before the cracks are fully formed, can preserve the hydrophilic surface, but removing the EGDPEA-*co*-DEGMA coating after the cracks are formed leads rapidly to the PDMS coverage of the

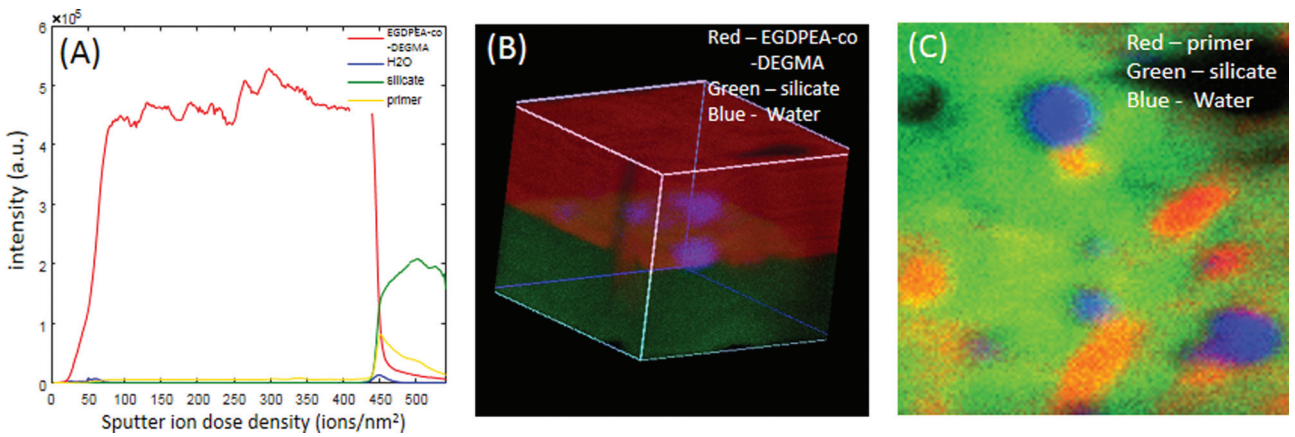


FIG. 12. ToF-SIMS depth profile (a), 3D image (b), and interface image (c) of the 100 × 100 $\mu$m region of the EGDPEA-*co*-DEGMA coated PDMS catheter that was treated for 5 min, with the $O_2$ plasma and then coated with the primer. Note that in the 3D image (b), the EGDPEA-*co*-DEGMA coating is shown in red, while in the interface image (c), red is used for the primer.

surface. This has important implications for the process development as well as forensic investigation of delaminated coatings.

The ToF-SIMS measurement of the 30 min treated sample showed increased PDMS, which is consistent with the high WCA measured on these samples. This film also showed a greater variation in the thickness of the polymer coating, associated with the surface cracks and holes. This suggests that the thinner coating, observed using gravimetric analysis, was the result of incomplete wetting of the surface at a microscale.

Cryo-ToF-SIMS analysis of the hydrated 10 min treated catheter revealed water disrupting contacts between the silicate and the EGDPEA-*co*-DEGMA layer over large portions of the surface. This suggests that the strong adhesion when dry was due primarily to easily hydrolyzed polar and hydrogen bonding interactions rather than covalent bonds.

In contrast, the sample treated with the primer showed only traces of water at the interface, which were likely associated with hydrophilic particulate contaminants, such as salt. Detection of water at the interface using cryo-ToF-SIMS proves that water is able to permeate the EGDPEA-*co*-DEGMA layer and access the interface but does not disrupt the adhesive bonds. This suggests that covalent bonding may be involved although no direct evidence for covalent bonding was found in the ToF-SIMS data. Evidence that hydrophilic dust particles may attract water to the interface suggests that future improvements in adhesion may be possible by reducing particulate contamination.

## IV. CONCLUSIONS

Dual-beam 3D imaging ToF-SIMS, using a 10 keV $Ar_{2000}^+$ cluster sputter source and a 30 keV $Bi_3^+$ analysis beam, was able to provide detailed information on the adhesive interface between the EGDPEA-*co*-DEGMA coating and the PDMS catheter. The polymer coating, PDMS, silicate, primer, and particulate contamination were identifiable in the interfacial region after sputtering through multiple micrometers of the polymer overlayer. Key components of the interface could be identified even in the presence of differential sputtering artefacts associated with surface particle contamination.

Oxygen plasma treatment of the PDMS catheter for 5–10 min resulted in efficient wetting of the catheter by the EGDPEA-*co*-DEGMA coating and good adhesion between the layers under dry conditions. Unfortunately, hydration, which is unavoidable in a urinary catheter, dramatically reduced the strength of the adhesive bond between the layers. Inclusion of a primer layer resulted in a more resilient adhesive bond between the EGDPEA-*co*-DEGMA and the PDMS catheter that was resistant to hydration. Although cryo-ToF-SIMS measurements could not directly confirm covalent bonding between the primed catheter and the coating, the ToF-SIMS measurements verified that adhesion persisted despite the presence of water at the interface. The resulting catheter material is resistant to bacterial biofilm colonization and has the mechanical properties necessary for use as a urinary catheter. Biofilm formation was reduced by between 86% and 95% in bacterial coverage for both *P. mirabilis* and UPEC compared to untreated PDMS and between 66% and 93% compared to the silver hydrogel after 10 days of continuous bacterial exposure. This study demonstrates the importance of Ar cluster depth profiling for the better understanding of adhesion between the polymeric layers and the development of improved biomaterials.

## ACKNOWLEDGMENTS

Funding from EMRP (IND56) is kindly acknowledged. Provision of the *P. mirabilis* strain from Roger Bayston is kindly acknowledged.

[1]T. M. Hooton *et al.*, Clin. Infect. Dis. **50**, 625 (2010).
[2]L. E. Nicolle, Infect. Dis. Clin. North Am. **26**, 13 (2012).
[3]P. Zarb *et al.*, Euro surveillance **17**, 20316 (2012).
[4]C. Chant, D. M. Smith, J. C. Marshall, and J. O. Friedrich, Crit. Care Med. **39**, 1167 (2011).
[5]C. M. Kunin, Q. F. Chin, and S. Chambers, J. Am. Geriatr. Soc. **35**, 1001 (1987).
[6]C. Clec'h *et al.*, Infect. Control Hosp. Epidemiol. **28**, 1367 (2007).
[7]D. J. Stickler and J. Zimakoff, J. Hosp. Infect. **28**, 177 (1994).
[8]P. Tenke, B. Kovacs, T. E. Bjerklund Johansen, T. Matsumoto, P. A. Tambyah, and K. G. Naber, Int. J. Antimicrob. Agents **31**, 68 (2008).
[9]A. L. Hook, C. Y. Chang, J. Yang, S. Atkinson, R. Langer, D. G. Anderson, M. C. Davies, P. Williams, and M. R. Alexander, Adv. Mater. **25**, 2542 (2013).
[10]A. L. Hook *et al.*, Nat. Biotechnol. **30**, 868 (2012).
[11]K. Adlington *et al.*, Biomacromolecules **17**, 2830 (2016).
[12]D. M. Siddiq and R. O. Darouiche, Nature Rev. Urol. **9**, 305 (2012).
[13]J. M. Leung, L. R. Berry, A. K. C. Chan, and J. L. Brash, J. Biomater. Sci.-Polym. Ed. **25**, 786 (2014).
[14]R. L. Williams, D. J. Wilson, and N. P. Rhodes, Biomaterials **25**, 4659 (2004).
[15]F. Abbasi, H. Mirzadeh, and A.-A. Katbab, Polym. Int. **50**, 1279 (2001).
[16]B. D. Ratner, A. Hoffman, and J. Whiffen, J. Bioeng. **2**, 313 (1978).
[17]T. R. Gengenbach, R. C. Chatelier, and H. J. Griesser, Surf. Interface Anal. **24**, 271 (1996).
[18]A. Parvin, H. Mirzadeh, and M. T. Khorasani, J. Appl. Polym. Sci. **107**, 2343 (2008).
[19]M. Seah, S. Spencer, R. Havelund, I. Gilmore, and A. Shard, Analyst **140**, 6508 (2015).
[20]T. B. Angerer, P. Blenkinsopp, and J. S. Fletcher, Int. J. Mass. Spectrom. **377**, 591 (2015).
[21]C. M. Mahoney and A. Wucher, *Cluster Secondary Ion Mass Spectrometry: Principles and Applications* (Wileyonline, New York, 2013), p. 117.
[22]M. Körsgen, A. Pelster, K. Dreisewerd, and H. F. Arlinghaus, J. Am. Soc. Mass Spectrom. **27**, 277 (2016).
[23]A. Pelster, B. J. Tyler, M. Körsgen, R. Kassenböhmer, R. E. Peterson, M. Stöver, W. E. Unger, and H. F. Arlinghaus, Biointerphases **11**, 041001 (2016).
[24]D. Rading, R. Moellers, H. G. Cramer, and E. Niehuis, Surf. Interface Anal. **45**, 171 (2013).
[25]H. Berger, J. Hacker, A. Juarez, C. Hughes, and W. Goebel, J. Bacteriol. **152**, 1241 (1982).
[26]J. L. Fritz and M. J. Owen, J. Adhes. **54**, 33 (1995).
[27]H. Hillborg, J. F. Ankner, U. W. Gedde, G. D. Smith, H. K. Yasuda, and K. Wikstrom, Polymer **41**, 6851 (2000).
[28]A. Karkhaneh, H. Mirzadeh, and A. R. Ghaffariyeh, J. Appl. Polym. Sci. **105**, 2208 (2007).
[29]A. I. Hidron, J. R. Edwards, J. Patel, T. C. Horan, D. M. Sievert, D. A. Pollock, S. K. Fridkin, National Healthcare Safety Network Team and Participating National Healthcare Safety Network, Infect. Control Hosp. Epidemiol. **29**, 996 (2008).

[30]K. Schumm and T. B. Lam, Cochrane Database Syst. Rev. **16**, CD004013 (2008).
[31]M. A. Robinson, D. J. Graham, and D. G. Castner, Anal. Chem. **84**, 4880 (2012).
[32]D. Breitenstein, C. E. Rommel, R. Mollers, J. Wegener, and B. Hagenhoff, Angew. Chem. Int. Ed. Engl. **46**, 5332 (2007).
[33]R. Peterson and B. Tyler, Appl. Surf. Sci. **203**, 751 (2003).
[34]R. E. Peterson and B. J. Tyler, Atmos. Environ. **36**, 6041 (2002).
[35]J. Roth *et al*., Langmuir **24**, 12603 (2008).
[36]E. C. Rangel, G. Z. Gadioli, and N. C. Cruz, Plasmas Polym. **9**, 35 (2004).
[37]See supplementary material at http://dx.doi.org/10.1116/1.4984011 for supporting graphics, images and spectra.